

IRON-BASED BAR – FE ALLOY – MODERN TIMES – FRANCE

Artefact name	Iron-based bar
Authors	Christian. Degriigny (HE-Arc CR, Neuchâtel, Neuchâtel, Switzerland) & Mathea. Hovind (University of Oslo, Department of archaeology, conservation and history (IAKH-UiO), Oslo, Oslo, Norway)
Url	/artefacts/881/

✧ The object



Fig. 1: Iron-based bar. Surface “a” and “b”, to the left and right, respectively,

Credit UiO-IAKH, M.Hovind.

✧ Description and visual observation

Description of the artefact	Iron-based bar with a circular pierced tip (Fig. 1). Its surface is covered by brown and orange-red corrosion products in addition to localized deposits of soil and charcoal. Dimensions: L = 374mm; W = 21mm; T = 6mm; WT = 293g.
Type of artefact	Not defined
Origin	Château de Germolles (14th century), Mellecey, Bourgogne, France
Recovering date	Unknown
Chronology category	Modern Times
chronology tpq	1801 A.D. ▼
chronology taq	1950 A.D. ▼
Chronology comment	19th - 20th century
Burial conditions / environment	Outdoor atmosphere
Artefact location	HE-Arc CR, Neuchâtel, Neuchâtel
Owner	Château de Germolles, Mellecey, Bourgogne
Inv. number	None.
Recorded conservation data	N/A

Complementary information

None.

Study area(s)

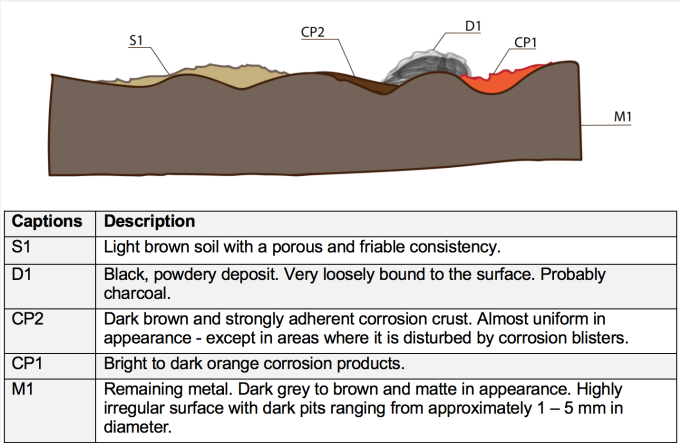


Credit UiO-IAKH, M.Hovind.

Fig. 2: Location of sampling area (a cross-section of the metal, marked by a stippled line),

Binocular observation and representation of the corrosion structure

The schematic representation below (Fig. 3) gives an overview of the corrosion layers encountered on the object from a first visual macroscopic observation.



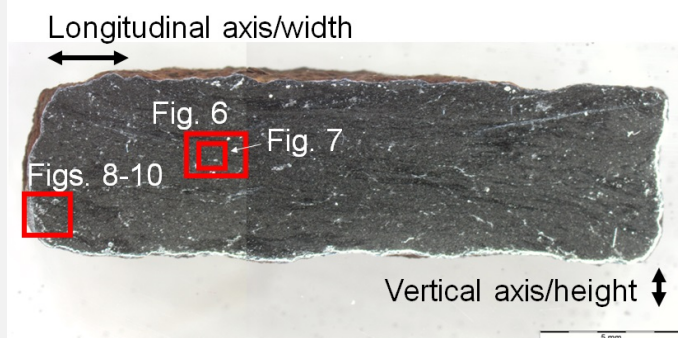
Credit UiO-IAKH, M.Hovind.

Fig. 3: Preliminary stratigraphy of the corrosion structure based on visual microscopic observation,

MiCorr stratigraphy(ies) – Bi

Sample(s)

Fig. 4: Micrograph of the cross-section of the iron-based bar with location of Figs. 6-10,



Credit UiO-IAKH, M.Hovind.

Description of sample	A rectangular section (Fig. 4) was cut out from the tip of the iron bar. Its longitudinal axis corresponds to the width of the iron bar while the height/thickness of the bar is represented by the vertical axis.
Alloy	Fe Alloy
Technology	Puddled iron
Lab number of sample	WIB2018 (Wrought Iron Bar sampled in 2018)
Sample location	HE-Arc CR, Neuchâtel, Neuchâtel
Responsible institution	HE-Arc CR, Neuchâtel, Neuchâtel
Date and aim of sampling	March 2018, study of corrosion stratigraphy and chemical analyses

Complementary information

The fact that the artefact was considered as test material enabled extensive sampling that would not otherwise be possible.

✧ Analyses and results

Analyses performed:

Metallography: microscope: Leica DMI8 (a metallographic, inverted, reflected light microscope) with magnification up to 500X. Camera: Olympus SC50 connected to the software "Olympus Stream", version 1.9.4. Illumination modes: bright field and cross-polarized light.

SEM-EDS: instrument: Jeol 6400; voltage: 20 kV; working distance: 18 and 24mm; sample preparation: palladium depot.

✧ Non invasive analysis

None.

✧ Metal

The metal is a wrought iron consisting of Fe, with some P and C (Fig. 5). The presence of Si is due to slag inclusions. The inclusions appear elongated* (Fig. 7) and filled with phases appearing light grey, medium grey and dark grey both in

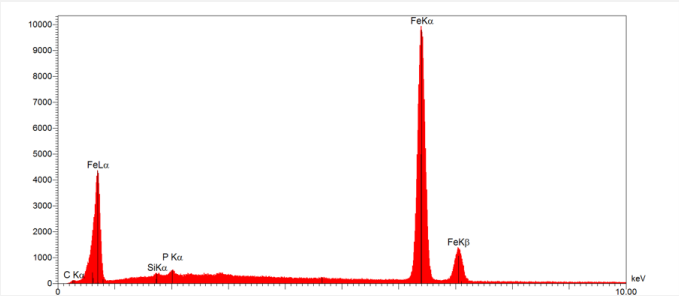
bright field and in SEM in BSE-mode (Figs. 6 and 7). Local analysis by SEM-EDS (Table 1) revealed that the light grey phase consists mainly of Fe and O with some C and has a composition similar to Wüstite (FeO). The medium grey phase has a similar composition but contains more P and C in addition to Si (Table 1). This phase is probably Wüstite in a Fe-P matrix. The dark grey phase corresponds to the glassy matrix and contains significantly higher concentrations of Si and P, in addition to the usual Fe and O (Table 1). The relatively high Si-content indicates that this phase might be Fayalite (FeSiO4) in a Fe-P matrix.

Smaller inclusions/nodules are evenly distributed throughout the metal (Fig. 6 and 7). They appear dark grey and have a composition similar to the dark grey phase in the elongated inclusions (Table 1).

Phase / nodule	Fe	O	P	Si	C	V	S	Mn	Al	Cr	Mg	Ca
Light grey phase	83	12	0.1	0.2	2	2	0.1	0.4	0.2	0.4	-	-
Medium grey phase	74	15	4	3	3	0.8	0.7	0.6	0.3	0.1	-	-
	52	22	13	8	3	-	0.2	-	0.1	-	0.2	0.1
Dark grey phase	49	27	11	5	6	-	1	0.9	0.1	-	-	-
Nodules												

Table 1: Chemical composition of the different phases in the slag inclusions and the nodules in the metal matrix. Method of analysis: SEM-EDS. Lab. of Electronic Microscopy and Microanalysis, Néode, HEI Arc, credit MiCorr_HEI Arc, C.Csefalvay.

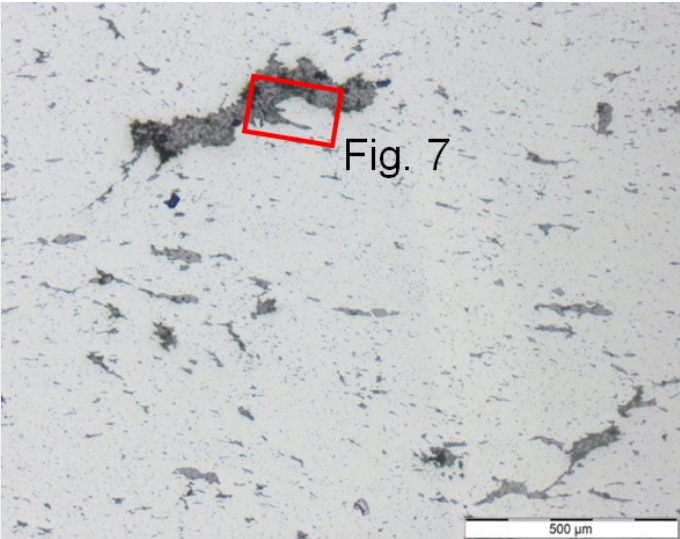
* As the section was cut across the iron bar – it is the cross section of the inclusions that are visible. Thus, their length and direction cannot be deduced directly from the sample.



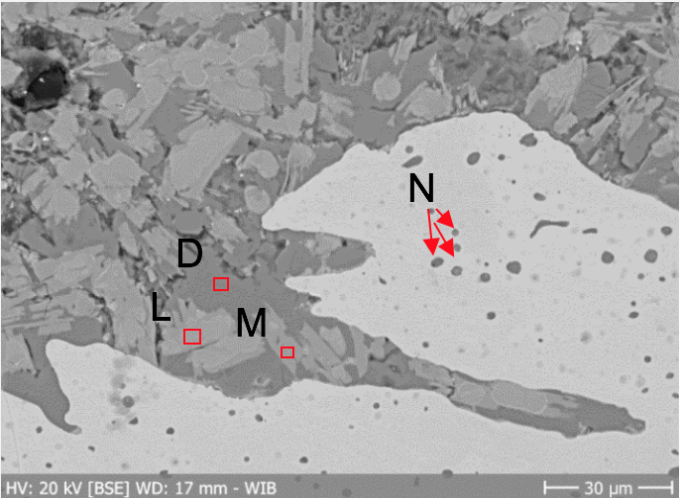
Credit HEI Arc, C.Csefalvay.

Fig. 5: EDS-spectrum showing the chemical composition of the metal (M1). The surface area analyzed was approx. 2*2 mm. Method of analysis: SEM-EDS. Lab. of Electronic Microscopy and Microanalysis, Néode, HEI Arc,

Fig. 6: Micrograph of the metal sample from Fig. 4 (detail), unetched, bright field. The microstructure of the metal with slag inclusions and the location of Fig. 7,



Credit UiO-IAKH, M.Hovind.



Credit HEI Arc, C.Csefalvay.

Fig. 7: SEM-image (BSE-mode) of the selected area from Fig. 6 (detail). The different phases in the slag inclusions are clearly visible: L = light grey phase, M = medium grey phase, D = dark grey phase/matrix, N = nodules,

Microstructure	Unknown
First metal element	Fe
Other metal elements	C, P

Complementary information

None.

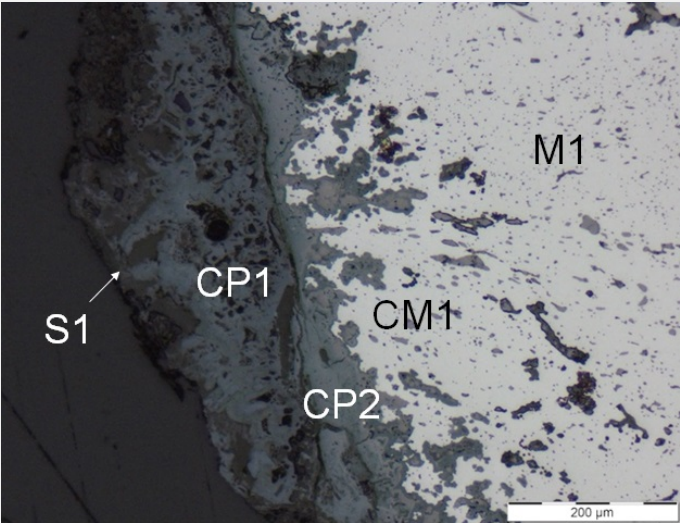
Corrosion layers

The corrosion crust is typical of exposure of iron to the atmosphere: it is relatively thick and consists of two layers: CP1 and CP2. The latter is a dense product layer appearing light grey under both bright field and polarized light (Figs. 8 and 9). The outermost layer (CP1) is a porous crust, appearing dark grey under bright field and bright orange under polarized light (Figs. 8 and 9). The corroded metal (CM1) appears as isolated areas of corrosion within the sound metal. The composition of the corrosion products shows a varying content of Fe and O throughout the crust with an increasing O-content towards the surface of the corrosion layer CP1 (Table 2). Elemental mapping by SEM-EDS (Fig. 10) shows that Ca and Mg are present in cracks which penetrates the outer corrosion crust (CP1). These elements are probably exogenous and could originate from the soil (S1) that is covering the metal surface.

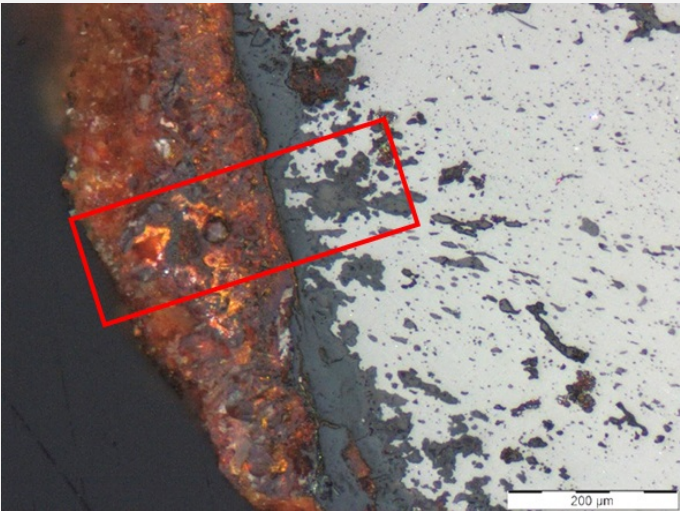
Elements mass %	Fe	O	C	Ca	Si	P	S	Mg	Al	V	Cr	Mn
Layer												

CP1	57	36	5	1.0	0.3	0.3	0.3	0.3	0.1	-	-	-
CP2	68	27	3	0.5	0.4	0.4	0.1	0.1	-	-	-	-
CM1	70	25	3	0.1	0.5	0.5	0.3	0.1	0.1	0.3	0.1	0.1

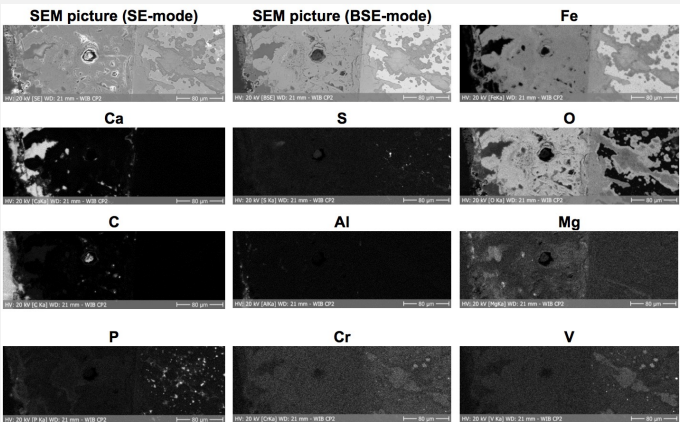
Table 2: Chemical composition of the corrosion layers from Figs. 8 and 10. Method of analysis: SEM-EDS. Lab. of Electronic Microscopy and Microanalysis, Néode, HEI Arc, credit MiCorr_HEI Arc, C.Csefalvay.



Credit UiO-IAKH, M.Hovind.



Credit UiO-IAKH, M.Hovind.



Credit HEI Arc, C.Csefalvay.

Corrosion form

Pitting

Fig. 8: Micrograph of the metal sample from Fig. 4 (detail), unetched, bright field to be compared to the stratigraphy representation of Fig. 11,

Fig. 9: Micrograph similar to Fig. 8, but under polarized light. CP1 in orange, CP2 and the corroded metal phase (CM) appear dark grey. The selected area for elemental chemical distribution (Fig. 10) is marked by a red rectangle,

Fig. 10: SEM image and elemental chemical distribution of the selected area from Fig. 9. Method of analysis: SEM-EDS. Lab. of Electronic Microscopy and Microanalysis, Néode, HEI Arc,

Corrosion type None

Complementary information

None.

✧ MiCorr stratigraphy(ies) – CS

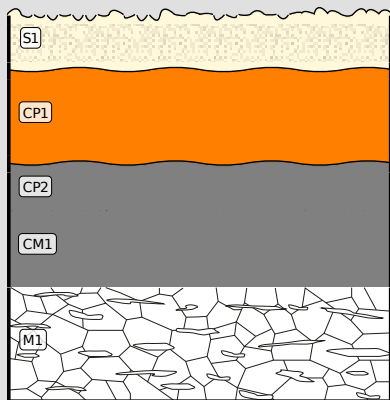
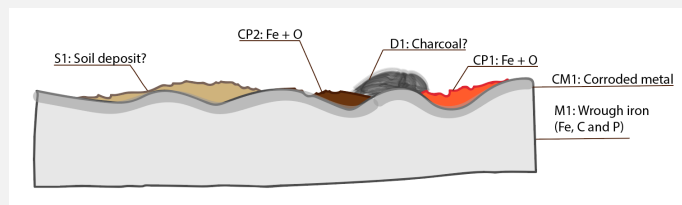


Fig. 11: Stratigraphic representation of the iron-based bar in cross-section (dark field) using the MiCorr application. The characteristics of the strata are only accessible by clicking on the drawing that redirects you to the search tool by stratigraphy representation. This representation can be compared to Figs. 8 and 9, Credit UiO-IAKH, M.Hovind.

✧ Synthesis of the binocular / cross-section examination of the corrosion structure

The schematic representation of corrosion layers integrating additional information based on the analyses carried out in Fig. 12.



Credit UiO-IAKH, M.Hovind.

Fig. 12: Improved stratigraphic representation of the iron-based bar based on analyses from cross-section and visual microscopic observation, CP = corrosion product, D = deposit, M = metal S = soil, CM = corroded metal,

✧ Conclusion

The artefact is a wrought iron with evenly distributed inclusions of what appears to be wüstite in a fayalite matrix. Wrought iron containing slags was readily available until World War II, after which it was substituted by low-carbon steels (Selwyn 2004:96). This indicates that the artefact can be dated no later than the first half of the 20th century. As regards the production method, it has been suggested (Dr. Phil. M. Senn, 2018, personal communication the 26th of April) that the artefact was produced by puddling, an indirect process for the conversion of pig iron to wrought iron, while decreasing the level of impurities (Selwyn 2004:112-113).

The corrosion products on the surface of the iron bar are typical for iron exposed outdoors with varying contents of Fe and O in addition to a layer of Ca-containing soil.

✧ References

References on object and sample

References sample

1. Selwyn, L. (2004) Metals and corrosion: A handbook for the conservation professional. Ottawa: Canadian Conservation Institute.